Coupled Interface Plasmons of Al Films on CdSe and CdS

Leonard J. Brillson
Xerox Webster Research Center, Webster, New York 14580
(Received 26 October 1976)

Coupled plasmon modes have been observed at interfaces of thin (3–100-Å) Al films with CdSe and CdS by low-energy electron energy-loss spectroscopy. The spectral features and their dependence on film thickness demonstrate that chemically reacted layers form at the metal-semiconductor junctions with frequency-dependent dielectric constants which are significantly different from their semiconductor counterparts.

In this paper, I report on the observation of coupled interface plasmon modes during the initial formation of metal-semiconductor junctions. While interface plasmon modes have been identified with various adsorbates on metals[1-3] or Si,[4,5] this is the first report of plasmon modes coupled between multiple media at atomic thicknesses. From low-energy electron energy-loss spectroscopy (ELS) of Al on CdSe and CdS as a function of metal film thickness, several interface modes could be identified and a frequency-dependent dielectric constant determined for the thin reacted layer formed at the metal-semiconductor interfaces.

Low-energy (100–500-eV) ELS was performed using a double-pass cylindrical-mirror analyzer and a grazing-incidence (20°) electron gun. Energy resolution was 0.8 eV. Second-derivative spectra of backscattered electrons were obtained from $(11\bar{2}0)$ CdSe and CdS crystals cleaved in ultrahigh vacuum (UHV) (base pressure $<8\times10^{-11}$ Torr). Submonolayer Al deposits were evaporated at pressures $<5\times10^{-10}$ Torr. Deposit thickness was monitored by a quartz-crystal device with a precision of 1 Hz corresponding to 0.7 Å. Surface chemical composition was measured by Auger electron spectroscopy (AES). Loss spectra were taken immediately after evaporation to minimize effects of any contaminants, which were always below the detectability limits of AES (<1% monolayer equivalent). AES measurements of Al coverage on CdSe or CdS indicated a sticking coefficient of ~1. Aluminum was particularly suited for this study because it forms smooth, continuous films at atomic thicknesses[6] and yields relatively uncomplicated ELS spectra.

ELS spectra of Al on CdSe are shown in Fig. 1. The cleaved $(11\bar{2}0)$ CdSe surface exhibits loss features associated with interband transitions at 3.0, 5.0, and 6.1 eV, a bulk plasmon at 17.2 eV, a Cd $4d$-level transition to the conduction-band density-of-states (DOS) maximum at 13.5 eV, and a 10.5-eV peak attributed to the CdSe surface plasmon. These energies agree with previous ELS measurements,[7] but their identification with surface versus bulk transitions may be more complex.[8] Evaporation of 2 Å of Al alters the CdSe ELS features. This deposition completely removes the ordered 1×1 low-energy electron-diffraction (LEED) pattern measured from the cleaved CdSe surface. Surface photovoltage spectroscopy (SPS) of CdSe[9] with 2 Å of Al showed no photoinduced work-function changes, thus indicating complete stabilization of the interface Fermi level. The 2-Å ELS features are unlike those of either the thick Al film or the CdSe substrate. The *LMM* Auger peak of Al occurred at 69 eV for the thick Al film but exhibited a chemical shift to 64 eV for

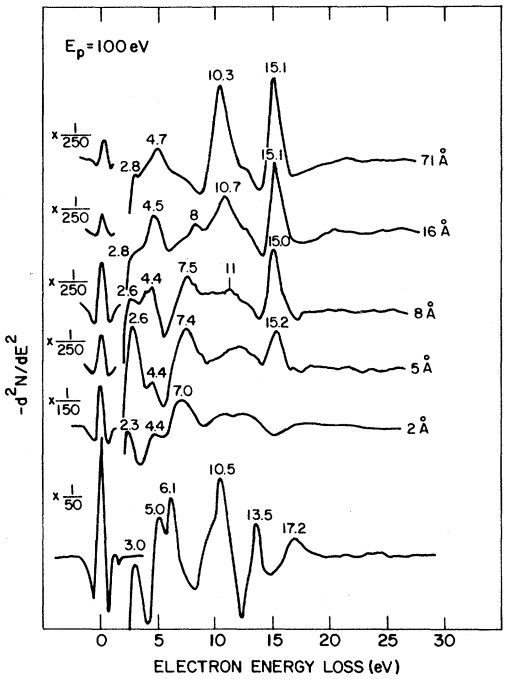

FIG. 1. Electron energy-loss spectra of Al deposited on cleaved $(11\bar{2}0)$ CdSe for various thicknesses of metal deposition.

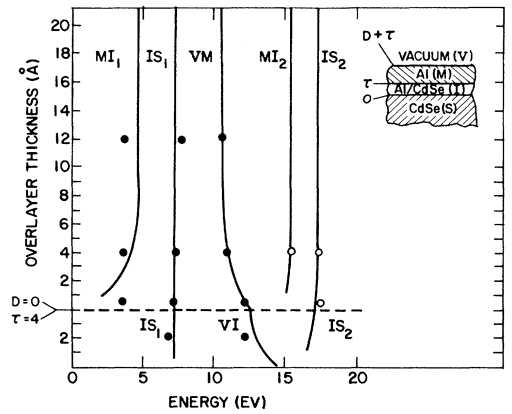

FIG. 2. Predicted ELS energies (solid lines) with $\omega_I = 14.0$ eV and $\Delta_I = 7.2$ eV for the above four-medium interface compared with the observed ELS peak energies (●) and unresolved structure (○) as a function of metal overlayer thickness. MI, IS, and MV label mode energies associated with the metal–reacted-layer, the reacted-layer–semiconductor, and the metal-vacuum interfaces, respectively.

2-Å Al on CdSe. ELS, LEED, SPS, and AES results all indicate that a chemical reaction occurs at the metal-semiconductor interface.

With increasing Al deposition, new ELS peaks appear which correspond to coupled plasmons of the metal-semiconductor interface as well as the bulk Al plasmon. All CdSe features are removed by the Al overlayer. With 5-Å deposition, a new peak appears at 15.2 eV which corresponds to the bulk plasmon of Al. This mode appears at a film thickness that is certainly less than 10 Å, allowing for slight thickness variation.[6] Thus, the bulk dielectric response of Al is evident even at these atomic thicknesses, a result anticipated by Stern and Ferrell.[10] Similar effects have been reported for Cs on W.[3] Furthermore the appearance of Al ELS features at 5 Å indicates that the reacted interface layer is only one or two monolayers thick.

Thicker Al films have a bulk plasmon frequency $\hbar\omega_p = 15.1$ eV near the zero–wave-vector value of 15.0.[11] The low apparent wave-vector dispersion in ELS backscattering is due to the $(1/K)^2$ dependence of electron scattering, the K^2 dependence of peak linewidth, and plasmon damping. Assisted by elastic diffraction,[12] the electron backscattering will be weighted toward the smallest possible change in wave vector $K_{\min} = \hbar\omega_p K(E_I)/2E_I = 0.38$ Å^{-1} versus incident wave vector $K(E_I) = 5.11$ Å^{-1} for incident beam energy $E_I = 100$ eV and plasmon energy $\hbar\omega_p = 15$ eV.

Additional peaks are seen at 4.5, 7.5, and 10–12 eV which shift in frequency and relative intensity with increasing film thickness. Additional unresolved structure may also be present between 15 and 20 eV at low metal thicknesses. The structure near 2.7 eV is believed to be characteristic bulk Al[13]; it appears in all ELS spectra of Al.

With the reacted interface layer, the metal-semiconductor junction can be viewed as a four-medium structure as shown schematically in Fig. 2. The effective dielectric constant of each medium has the form[14] $\epsilon_i = 1 + \omega_i^2/(\Delta_i^2 - \omega^2)$, where $\omega_M = 15.1$ eV and $\Delta_M = 0$ for Al, $\omega_S = 17.2$ eV and $\Delta_S = 7.85$ eV for CdSe (assuming a low-frequency dielectric constant[15] $\epsilon_0 = 5.8$), $\omega_V = 0$ for vacuum, and ω_I and Δ_I are fitted parameters for the dielectric constant of the interface layer. From the continuity of normal electric displacement and transverse electric field across the boundaries, one obtains the equation, valid for $K \gtrsim K_{\min} \gg \epsilon_i^{1/2}\omega/c$

$$\frac{1-\delta e^{-2k\tau}}{1+\delta e^{-2k\tau}} \frac{\gamma e^{-2kD}+1}{\gamma e^{-2kD}-1} \frac{\epsilon_I}{\epsilon_M} = 1, \qquad (1)$$

where $\gamma = (\epsilon_M - 1)/(\epsilon_M + 1)$, $\delta = (\epsilon_I - \epsilon_S)/(\epsilon_I + \epsilon_S)$, D is the metal overlayer thickness, and τ is the reacted layer thickness equal to 4 Å since a bulk Al plasmon appears at $D + \tau = 5$ Å. Analogous expressions for three-layer structures have been derived previously.[10,16] The solutions of Eq. (1) can be identified with the various boundaries from roots of the equations $\epsilon_i = -\epsilon_j$ valid in the limit of large k, for each set i,j of semi-infinite adjoining media.[17] This identification is possible because of the low dispersion at large wave vector. Given the form of ϵ_M, ϵ_I, and ϵ_S, Eq. (1) has five solutions. These are labeled VM, $(MI)_1$, $(MI)_2$, $(IS)_1$, and $(IS)_2$ for the boundaries between vacuum (V), metal (M), reacted layer (I), and semiconductor (S). By varying only ω_I and Δ_I to fit these solutions to the experimental peak positions in Fig. 1, one obtains $\omega_I = 14.0$ eV and $\Delta_I = 7.2$ eV. The roots of Eq. (1) with this ω_I and Δ_I fit yield the energy-versus-thickness dependence shown in Fig. 2. As shown, the frequencies quickly converge to thick-film limits, characteristic of the large–wave-vector scattering. The observed modes near 4.5, 7.5, and 10.3 eV show close agreement with three of the fitted curves. A small peak near 17.2 eV can be seen only in the 5- and 8-Å spectra of Fig. 1. The 17.2- and 7.5-eV modes associated with the IS boundary are attenuated by the thickening metal overlayer. The 15.6-eV mode may lie in the shoulder of the 15.1-

eV bulk plasmon.

The 7.5-eV mode is evidence for an interface layer with $\epsilon_I \neq \epsilon_S$ or ϵ_M, since the modes calculated for a vacuum/bulk Al/CdSe structure lie at 4.8, 10.7, and 17.3 eV. In addition, the solutions of Eq. (1) cannot be fitted to the observed peaks with a frequency-independent ϵ_I. Associating the 10.3-eV peak with the VM interface since the Al surface plasmon energy $\hbar\omega_p/\sqrt{2} = 10.7$ eV, one obtains no reasonable, self-consistent $\epsilon_I \neq \epsilon_I(\omega)$ to account for the other ELS peaks.

Ritchie[18] and Schmüser[1] have discussed the two coupled modes of a semi-infinite metal film bounded by dielectric media. For $E_B = 100$ eV, $K \leq K(E_B)$, and thickness D greater than several angstroms, the intensity ratio of the higher-energy (+) mode to the lower-energy (−) mode is

$$\frac{I_+}{I_-} \simeq \frac{1-\cos(D\hbar\omega_p K/\sqrt{2}E_B)}{1+\cos(D\hbar\omega_p K/\sqrt{2}E_B)}. \quad (2)$$

This ratio increases thickness and decreases with increasing energy as the coupling strength changes between the electron beam and the electric fields of each plasmon mode. This qualitative behavior is independent of the bounding dielectric media. For monolayer thicknesses of Al, $I_+/I_- \sim 1$ at 100 eV but $I_+/I_- \ll 1$ at transmission ELS energies.

Figure 1 shows an increase in the intensity ratio $I(\omega_{VM} = 10.3\text{ eV})/I(\omega_{MI_1} = 4.5\text{ eV})$ with increasing film thickness, in qualitative agreement with Eq. (2). The absence of well-defined MI_2 and IS_2 modes may also be due to their weaker coupling to the electron beam than the MI_1 and IS_1 modes. The decrease in $I(\omega_{IS_1})/I(\omega_{VM})$ with increasing thickness can be accounted for by overlayer attenuation. The metal film thickness can be estimated independently from $I(\omega_{VM})/(\omega_{MI_1})$ and Eq. (2). For a 16-Å deposit equivalent to $D \sim 12$ Å plus $\tau = 4$ Å, one obtains a comparable metal film thickness $D = 7$ Å from $I(10.7\text{ eV})/I(4.5\text{ eV}) = 1.5$. A scattering wave vector $K = 0.2$ Å^{-1} was used to fit the ω_{VM} dispersion in Fig. 2. This value is consistent with the low dispersion of the bulk Al plasmon.

An important consequence of the ω_I and Δ_I fit is that the low-frequency dielectric constant is $\epsilon_I(0) = 1 + \omega_I^2/\Delta_I^2 = 4.9$ versus 5.8 for CdSe.[13] Therefore the dielectric constant of the reacted interface layer is significantly lower than that of the semiconductor substrate. Small changes on the fit of ω_I and Δ_I do not alter this result. The lower $\epsilon_I(0)$ is consistent with formation of a more ionic interface compound, similar to Al_2O_3 [$\epsilon(0) = 3.1$], since the plasmon energy $\hbar\omega_I$ is reduced. Al_2Se_3 chemical shifts are unavailable for identifying this compound. However, it should not be stoichiometric Al_2Se_3 because of the Cd atoms which intervene. Intentional oxidation of thick (100 Å) Al films produced spectra like those of Powell and Swan,[2] with mode energies and thickness dispersion unlike the metal-semiconductor results.

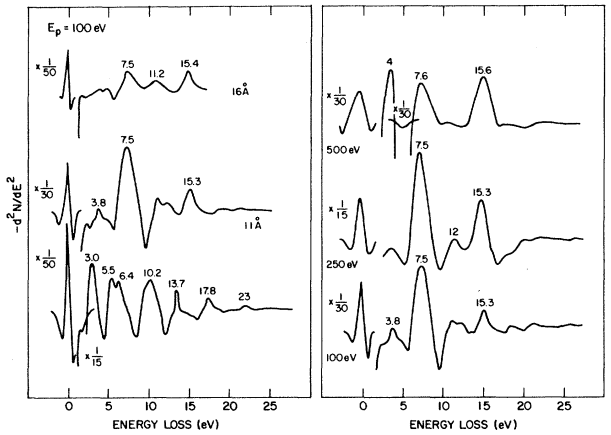

FIG. 3. (a) Electron energy-loss spectra of Al deposited on cleaved (11$\bar{2}$0) CdS for various thicknesses of metal deposition; (b) electron energy-loss spectrum of 11-Å Al on CdS for various incident beam energies.

Figure 3(a) illustrates the ELS spectra for Al on cleaved (11$\bar{2}$0) CdS. Again the cleaved surface exhibits loss peaks corresponding to interband transitions at 3.0, 5.5, and 6.4 eV. These are shifted up slightly because of the larger band gap. As with CdSe, a Cd 4*d*-level transition to the conduction-band DOS maximum is observed at 13.7 eV as well as a bulk plasmon at 17.8 eV and a surface plasmon at 10.2 eV. With Al deposition, this spectrum is completely altered, giving rise to new structure at ~4, 7.5, and ~11 eV, analogous to the Al/CdSe spectra. The emergence of the Al bulk plasmon mode, the increase of the $I(\omega_{VM} \simeq 11\text{ eV})/I(\omega_{MI_1} \simeq 4\text{ eV})$ peak ratio, and the decrease of ω_{VM} with increasing thickness follow the Al/CdSe analysis of Fig. 1. Furthermore, with a CdS $\epsilon(0) = 5.5$,[13] one obtains $\epsilon_I(0) = 5.0$, again lower than that of the semiconductor substrate. Figure 3(b) shows the effect of primary beam energy on the ELS spectra of 11-Å Al/CdS. With increasing energy, the $\omega_{MI_1} = 4$ eV and $\omega_{IS_1} = 7.6$ eV modes increase relative to the $\omega_{VM} = 11$ eV mode, in qualitative agreement with Eq. (2) and the increased electron escape depth. The bulk plasmon intensity also increases relative to $I(\omega_{VM})$ as more of the bulk is probed.

In summary, coupled plasmon modes have been observed at chemically reacted metal-semiconductor contacts, and interface dielectric constants could be determined from the ELS features.

I am indebted to C. B. Duke for considerable assistance and encouragement with the theoretical analysis and to J. J. Ritsko and E. M. Conwell for many stimulating discussions.

[1]P. Schmüser, Z. Phys. 180, 105 (1964).
[2]C. J. Powell and J. B. Swan, Phys. Rev. 118, 640 (1960).
[3]A. U. MacRae, K. Muller, J. J. Lander, J. Morrison, and J. C. Phillips, Phys. Rev. Lett. 22, 1048 (1969).
[4]B. Goldstein, Surf. Sci. 35, 227 (1973).
[5]H. Ibach and J. E. Rowe, Phys. Rev. B 9, 1951 (1974).
[6]L. Holland, *Vacuum Deposition of Thin Films* (Chapman and Hall, Ltd., London, 1963), p. 207.
[7]R. L. Hengehold and F. L. Pedrotti, Phys. Rev. B 6, 2262 (1972).
[8]C. B. Duke, A. R. Lubinsky, M. Bonn, G. Cisneros, and P. Mark, Sci. Technol. 14, 294 (1977).
[9]L. J. Brillson, J. Vac. Sci. Technol. 13, 325 (1976).
[10]E. A. Stern and R. A. Ferrell, Phys. Rev. 120, 130 (1960).
[11]P. C. Gibbons, S. E. Schnatterly, J. J. Ritsko, and J. R. Fields, Phys. Rev. B 13, 2451 (1976).
[12]C. B. Duke and G. E. Laramore, Phys. Rev. B 3, 3183 (1971).
[13]E. Petri and A. Otto, Phys. Lett. 34, 1283 (1976).
[14]R. G. Barrera and C. B. Duke, Phys. Rev. B 13, 4477 (1975).
[15]M. Cardona and G. Harbeke, Phys. Rev. 137, A1467 (1965).
[16]J. W. Gadzuk, Phys. Rev. B 1, 1267 (1970).
[17]Effects of electron density profiles at these wave vectors for Al are slight. See P. J. Feibelman, Phys. Rev. Lett. 30, 975 (1973).
[18]R. H. Ritchie, Phys. Rev. 106, 874 (1957).

Theory of Angle-Resolved Photoemission from Ordered Overlayers

Ansgar Liebsch
Institut für Festkörperforschung, Kernforschungsanlage, 517 Jülich, Germany
(Received 29 October 1976)

Theoretical energy distributions are presented for ultraviolet photoemission from the valence states of an ordered (1×1) oxygen monolayer adsorbed on a (001) Ni surface. The spectra show the expected oxygen $2p$ resonances which are split and broadened as a result of the hybridization with the Ni conduction bands. Their intensity and shape depend strongly on the detector angles and the polarization of the incident light.

A new approach to photoemission from ordered overlayers adsorbed on a semi-infinite substrate is introduced. Its aim is the investigation of how the electronic structure of chemisorption systems manifests itself in the observed spectra. As an example of the kind of information the approach can give, calculations for the emission from $2p$ valence levels of a (1×1) oxygen layer on Ni(001) are presented. These results show the following features: (a) The adsorbate resonances are broadened and split because of the hybridization with the substrate conduction bands; (b) the oxygen levels show a dispersion and additional splitting as a result of the interaction between adatoms; (c) the resonances depend very differently on the polarization of the incident light because of their characteristic orbital symmetry; and (d) strong final-state effects demonstrate that the energy distributions are not proportional to the local density of states.

The excitation of the photoelectron is considered as a one-step process,[1] initial and final states being derived from the same one-electron Hamiltonian. To evaluate the initial state, I solve first for the complex band structure of the Ni substrate. The propagating and evanescent Bloch waves together provide an adequate expansion set for the stationary ground state inside the bulk. This function is subsequently matched to appropriate overlayer states and solutions to the external potential. I use a muffin-tin potential with the self-consistent Wakoh[2] potential for the Ni substrate and an atomic $X\alpha$ potential ($\alpha=0.744$) for the oxygen overlayer. In the vacuum, the potential is assumed to depend only on the coordinate z normal to the surface. I take an image form such that it continues at the adsorbate-vacuum interface into the inner potential. The oxygen atoms are adsorbed in the centered positions and the Ni-O bond length is taken from recent low-ener-